Scientific Justification

The remit of Galactic Archaeology is to leverage chemo-chrono-dynamical information from Milky Way stellar populations to generate robust z=0 constraints on galaxy formation theory. Reconstructing the history of star formation and mass assembly of the Galaxy from the fossil record opens a window into the physics of the early Universe. The time is ripe for chemo-chrono-dynamical data for statistically significant stellar samples to be extended to other galaxies, spanning a range in mass, morphology, and environment. The Local Group is the necessary starting point for that journey. We propose a pilot program to initiate an exploration of the chemical properties of resolved *old* stars in the disk of the Triangulum galaxy (M33), the nearest undisturbed massive dwarf. *Dwarf galaxies are crucially important: i*) they are the most abundant types of galaxies in the Universe; *ii*) due to downsizing (Cowie et al., 1996) they dominate star formation at z=0; *iii*) they are the z=0 counterparts of the early building blocks of massive galaxies, so their oldest stellar populations retain vital clues on the initial stages of galaxy assembly. *We will use NIRSpec spectroscopy to measure precise elemental abundances and relative ages for hundreds of red giant stars in the disk of M33.* These data will shed new light into the early history of star formation and mass assembly of one of the most interesting and mysterious dwarf galaxies in the Local Group.

1 Why Extra-Galactic archaeology

Galaxies are extremely diverse systems, whose properties depend on mass, environment, dark matter content, and morphology. Global galaxy properties have been mapped by several giant extragalactic surveys covering a range of lookback times. Their main limitation is the lack of detailed information on a galaxy by galaxy basis. Conversely, massive spectroscopic surveys of the MW have revolutionised our understanding of its history of formation and evolution by providing detailed chemodynamical information for $\sim 10^6$ stars. However, despite the tremendous power of chemodynamics for massive stellar samples, it has thus far only been able to afford robust tests for the Milky Way (MW) and a scant handful of the very nearest galaxies. Bridging the gap between these two extremes is crucial for a theoretical formulation of galaxy formation that unifies the existing evidence at all scales. We propose to take initial steps in that direction by capitalizing on the formidable amplification of observational capabilities offered by JWST to extend the reach of precision galactic archaeology beyond the MW and its satellites. The Triangulum galaxy (M33) is the ideal candidate for starting this journey while providing a great opportunity to further our understanding of dwarf galaxy formation and evolution.

2 Why M33

With a comparable stellar mass to the Large Magellanic Cloud ($M_\star$ $\sim$1-3$\times10^9$ $M_\odot$; e.g., van der Marel et al., 2002; Carrera et al., 2008; van der Marel et al., 2012; Beasley et al., 2015), M33 is the most massive satellite of Andromeda and one of the most massive satellite galaxies in the Local Group. It is classified as a disk galaxy that lacks a significant bulge component (Kormendy & McClure, 1993; McLean & Liu, 1996), has been observed to host a weak bar (Elmegreen et al., 1992; Regan & Vogel, 1994; Block et al., 2004; Corbelli & Walterbos, 2007), and has recently been postulated to contain a relatively compact stellar

halo (Gilbert et al., 2022). In addition, due to its relatively low stellar surface density, M33 stellar populations are more easily resolvable than those in other Local Group galaxies at similar distances, such as M31 and M32. In fact, M33's proximity allows us to resolve stars down to the ancient main sequence (Williams et al., 2009).

Several previous attempts have been made to determine elemental abundance ratios for *young* giant stars in the disk of M33 (e.g., McCarthy et al., 1995; Monteverde et al., 1997, 2000; Urbaneja et al., 2005; Rosolowsky & Simon, 2008; Cioni, 2009; Peña & Flores-Durán, 2019), confirming a metallicity gradient previously conjectured with other techniques (e.g., Searle, 1971; Kwitter & Aller, 1981; Vilchez et al., 1988; Garnett et al., 1992; Crockett et al., 2006). Despite these achievements, there is very little knowledge on the chemical properties of *old* populations in M33, and little known about its early star formation history. The ability to determine elemental abundance ratios for older giant stars with JWST will provide the vital and necessary data to tackle these problems. Similarly, these data will allow for an unprecedented comparison with theoretical expectations from state-of-the-art cosmological numerical simulations. These seem to suggest that galaxies of masses similar to M33 are undergoing high rates of average star formation (Muñoz-Mateos et al., 2007; Tollerud et al., 2011), which is at odds with the cosmological expectation that infalling satellites should experience little star formation via quenching. Finally, spectroscopic studies have unveiled the presence of a kinematically distinct population likely associated with an old, dynamically hot stellar halo (Gilbert et al., 2022).

In light of all the evidence, M33 makes for an interesting target to study the distribution of old stars in chemical composition space. Our strategy is to dedicate a modest amount of observing time to obtain high signal-to-noise (S/N) Near-Infrared (NIR) spectra of bright giants selected from a carefully chosen field. These will be used to determine, for the first time, the detailed abundance pattern of hundreds of M33 stars. Such data must hold the fundamental clues to M33's histories of star formation and chemical enrichment, and of its history of interaction with M31.

3 Constraining M33's star formation history with stellar chemistry

The global aspects of the cosmic history of star formation and chemical enrichment have been well documented in studies of galaxy populations in integrated light, both in the nearby universe (e.g., Kauffmann et al., 2003; Brinchmann et al., 2004; Blanton, 2006; Salim et al., 2007; Goddard et al., 2017) and at intermediate redshifts (e.g., Bundy et al., 2006; Noeske et al., 2007; Faber et al., 2007; Martin et al., 2007; Zahid et al., 2012). Correlations between mass and the light-weighted mean ages, metallicities, and ratio between the abundances of α-elements and Fe ([α/Fe]) have been established (Worthey et al., 1992; Walcher et al., 2015; Martín-Navarro, 2016; Zheng et al., 2019). The latter observable provides a measure of the ratio between the contributions of type II and type Ia supernovae to chemical enrichment (e.g., Tinsley, 1979; Matteucci & Greggio, 1986; McWilliam, 1997), and thus is an ideal tracer of star formation activity. Its correlation with galaxy mass suggests the presence of an interplay between cooling and feedback in the hearts of massive dark matter halos (e.g., Governato et al., 2015; Maoz & Graur, 2017; Gebek & Matthee, 2022). To disentangle the intricacies of this process one needs to retell the detailed history of star formation of galaxies, which is possible through determining the detailed chemical properties of their resolved stellar populations. Furthermore, these properties must be mapped in systems spanning the full

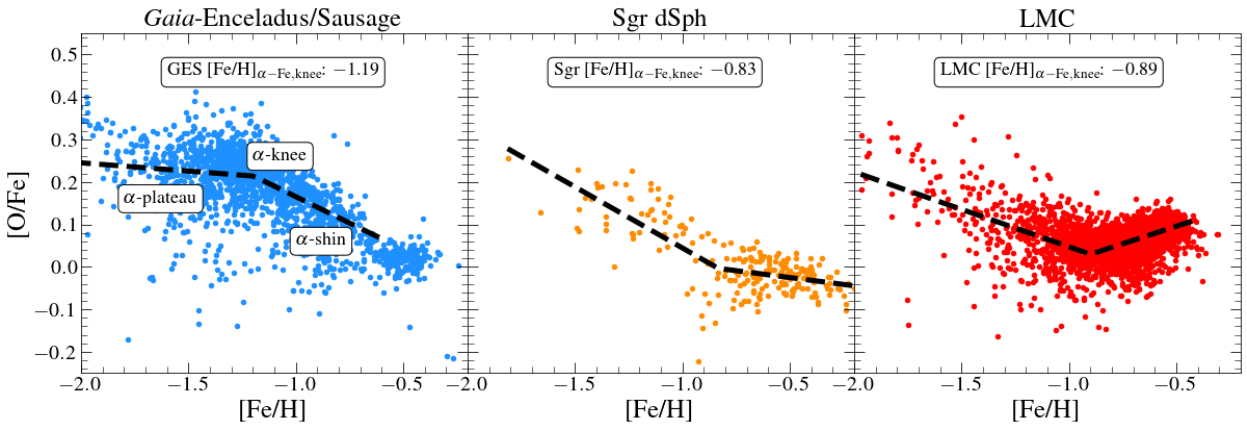

Figure 1: [O/Fe]-[Fe/H] distribution for three satellite galaxies of the MW with similar mass to M33 using APOGEE DR17 red giant data. *Left*: *Gaia*-Enceladus-Sausage, *middle*: Sgr dSph, *right*: Large Magellanic Cloud. Plotted as a black dashed line is a piece-wise linear model fitted to the data, where the break corresponds to the α-Fe knee, listed also in the box. As can be seen from these three examples, the metallicity of the knee and the morphology of the α-Fe plane varies for different dwarf galaxies, that is ultimately linked to the early star formation history of these systems.

range of global properties (mass, dark matter content, environment, morphology) so that theoretical predictions can be tested under all relevant sets of boundary conditions. Here we propose to take initial steps towards obtaining such crucial data for M33.

The distribution of the stellar populations of galaxies in the [α-Fe]-[Fe/H] (α-Fe) plane is a powerful indicator of star formation history. In the dwarf galaxy regime, [α/Fe] is typically lower than for larger-mass systems (like the MW, see for example Tolstoy et al., 2009 and references therein), likely because they expelled much of their star forming gas after the first episodes of star formation. So far, the α-Fe has been mapped in some detail in MW satellites (e.g., Hayes et al., 2020; Nidever et al., 2020; Hasselquist et al., 2021; Horta et al., 2022; Fernandes et al., 2023) where it is found to vary strongly from system to system, clearly indicating that the early chemical evolution and star formation of dwarf galaxies has been complex (Fig 1). In some cases, the distribution shows a clear plateau+knee structure (e.g., GES/Sausage), whereas in other cases there is a clear turnover towards constant or even increasing [α/Fe] (Sgr dSph and LMC, respectively). In more massive systems, such as the MW disk, a bimodal distribution on the α-Fe plane has been shown to exist (e.g., Hayden et al., 2015; Mackereth et al., 2017). While there is a clear correlation between the detailed chemistry and galaxy mass (e.g., Tolstoy et al., 2009; Hendricks et al., 2014), the large scatter in this correlation (e.g., Nidever et al., 2020) suggests the influence of additional variables (e.g., Fernandes et al., 2023).

The data we seek to obtain for M33 stellar populations will help establish where in the spectrum of known distributions on the α-Fe plane (or beyond it) M33 is located, and in turn it will teach us how its history of star formation compares with those of the MW and its satellites. Does M33 display a classical α-knee such as that detected in GES (Fig 1) and other dwarf galaxies? If so, does it occur at the metallicity expected on the basis of its stellar mass, or does it depart strongly from existing empirical correlations (Hayden et al., 2015; Mackereth et al., 2017), indicating a SFH that departs strongly from those of MW satellites (Hasselquist et al., 2021)? Have the more recent star formation brought about a substantial change in the α-Fe plane such as observed in, e.g., the Sgr dSph and the LMC (Fig. 1)? What will the SFH implied by these data tell us about the history of interaction

between M33 and its giant host M31? Perhaps even more interestingly, does M33 display a bimodality in [α/Fe] as manifested in the MW disk?

4 Precision chemistry in M33 with NIRSpec

Benefiting from the spatial resolution, low background, and multi-object spectroscopic capabilities of JWST, we will begin to chart out the chemical composition map of the disk of M33. For this pilot study, we will target a field in the outskirts of the M33 disk, to derive precision abundances of a multitude of elements covering various nucleosynthetic pathways (SNe II, SNe Ia, AGB). Critical abundances such as those of Fe-peak elements Fe, Mn, Cr, and Ni, α elements Mg, Ca, Ti, and Si, odd-Z elements Al and Na will be estimated on the basis of atomic lines that will be detected at the expected S/N and instrumental resolution (Section 4). Very importantly, molecular bands due to CN, CO, and OH will make possible the determination of the abundances of light elements C, N, and O. By applying chemical evolution modelling techniques which have been honed on the analysis of MW stellar populations (e.g., Andrews et al., 2017; Rybizki et al., 2017; Johnson et al., 2021), we will address the following key science questions: *i*) is there an [α/Fe] knee and/or [α/Fe] bimodality in the old M33 disk?; *ii*) what was the early history of star formation of the M33 disk? *iii*) what is the age distribution of M33 old disk stars? The elemental abundances alone will provide answers to (i) and (ii), whilst the inclusion of relative age estimations based on C and N abundances (described below) will lend insights into (iii).

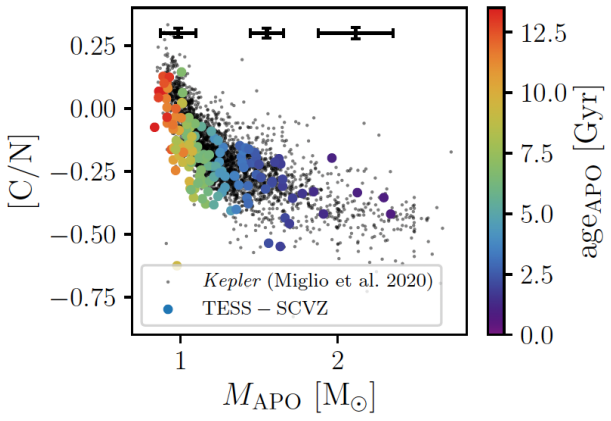

Figure 2: Asteroseismic Mass vs [C/N] ratio, coloured by age estimate for APOGEE giants in TESS and Kepler. At ∼1 $M_\odot$, a change in mass of ∼0.2 $M_\odot$ corresponds to a change in [C/N] of ∼ 0.2 dex, and an age difference of ∼2 Gyr.

JWST offers the only available means for this project. Ground based attempts are limited by crowding to the outskirts of the M33 disk and deliver relatively low precision. JWST's spatial resolution is key to overcoming crowding. The ability of NIRSpec to cut through dust extinction and background contamination yields the high S/N required for precision abundance determinations with relatively short exposure times. In the 0.9-1.8 μm regime, such abundances can be well constrained in cool giant spectra from modelling of atomic lines and molecular bands. The ability of JWST to observe in the NIR without being affected by absorption features in the Earth's atmosphere, also allows vast increases in achievable S/N, since the spectro-photometry is not limited to the J,H,K bands.

Besides assessing the presence of the [α/Fe] knee and/or bi-modality, we will constrain the star formation history of the old M33 disk by measuring relative stellar ages. There is a great precedent for age determinations from CNO abundances in MW disk giants (Fig. 2). The by-products of the CNO cycle that are dredged up to the stellar surface are a function of main sequence mass (Salaris et al., 2015). Thus, these elements are key indicators of stellar age in red giant stars (e.g., Martig et al., 2016; Ness et al., 2016). This relative age diagnostic, in addition to the C, N, O, and Fe abundances, will be pivotal for further understanding

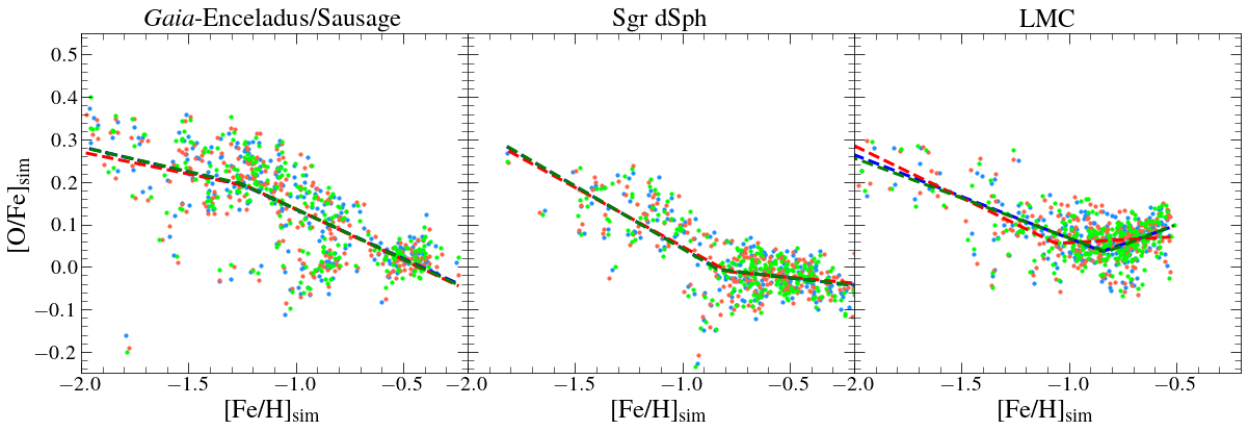

Figure 3: The same as Fig 1, but now for three mock data sets simulated by sampling 200 times the [Fe/H] and [O/Fe] abundance for a sample of 250 stars in each dwarf (randomly selected) assuming a 0.1 dex error, and then repeating the piece-wise linear fit to the resulting median value. Our ability to measure the α-knee is preserved assuming these abundance errors.

star formation in lower-mass galaxies, for deciphering the different star-formation episodes in M33 due to its interaction with Andromeda, and for unveiling its history of mass assembly.

Finally, combining abundances of C, N, O, Na, Mg, and Al will help in identifying globular cluster escapees in the M33 field population, which may be detected if their fractional contribution to the field is similar to estimates for the MW (e.g., Koch et al., 2019; Horta et al., 2021)

5 Expanding the galactic archaeology "repertoire"

It is unlikely that the study of galactic archaeology will be possible much further outside the Local Group within the near future. At larger distances, only photometric and integrated light studies will be viable in determining chemical features such as the α-Fe knee and/or element bimodality in extra-Galactic sources, especially in dwarf galaxies. This is another very important reason why stellar spectroscopy in M33 is one of the most important frontiers in galactic astrophysics: in order to attain maximal impact in distant photometric and integrated-light studies, we need to grow a galactic archaeology repertoire. M33 is an essential asset to this repertoire, after the MW and its satellites, since it is an excellent testing ground for photometric and integrated-light work, where individual spectroscopic targets are also observable. Our study and subsequent spectroscopic censuses of M33 will be an important pilot towards the best training data for such approaches. In summary, using the proposed using multi-object NIR spectroscopy with NIRSpec, this pilot study will:

1. Measure the detailed abundance pattern of 140 red giant stars in the old disk of M33, establishing the distribution of M33 stars in multi-dimensional chemical space.

2. Establish the age distribution of old stars in the M33 disk.

3. Detect M33 halo stars, measuring their detailed chemical compositions.

4. On the basis of the above data constrain the early history of star formation and mass assembly of M33.

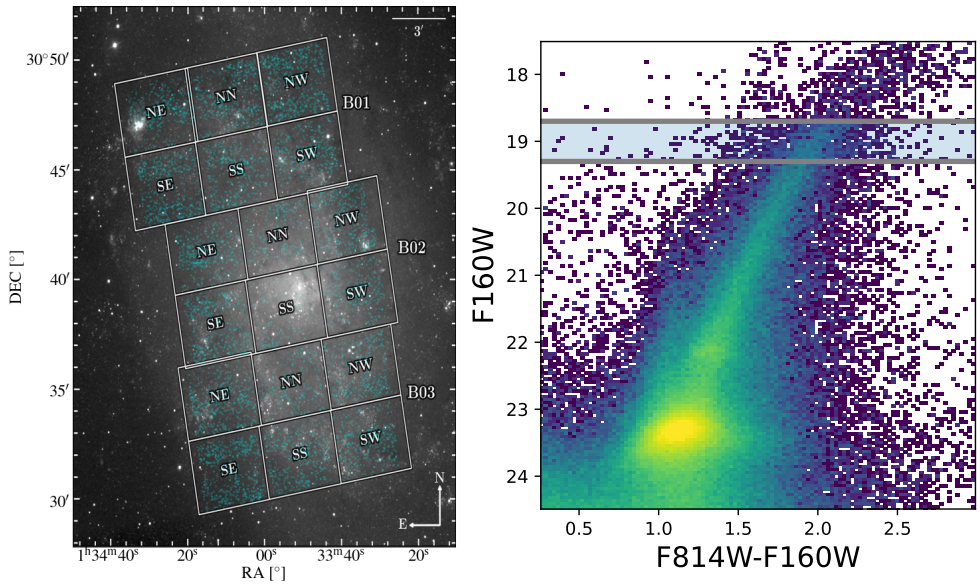

Figure 4: (a): Targets from the PHATTER survey we aim to observe superimposed over the footprint from Williams et al. (2021). **(b)**: Colour-magnitude diagram for evolved stars in the B01 NW brick we aim to target.

This project will lay foundations for a future program aimed at mapping the elemental abundance patterns across the entire disk and halo of M33. Our long term goal is to perform the *chemical cartography* of Local Group galaxies, ushering in a new era in the field of galactic archaeology.

Technical Justification

Goal: We propose to obtain medium resolution, high S/N, spectra for 140 bright M33 disk red giants within a narrow range of $T_{\rm eff}$ and log g. The spectra will be used for the derivation of precision elemental abundances, which will enable the determination of the distribution of old M33 disk stellar populations in age and chemical composition planes.

The data analysis will proceed in two complementary ways: (i) Combining synthetic distributions of stellar populations in various chemical/age planes, state of the art model atmospheres and spectrum synthesis, and an error model, we will forward model the distribution of spectral features for comparison with our measurements. The input distributions will include both theoretical predictions from numerical simulations and APOGEE-based observations of dwarf MW satellites (Fig. 3); (ii) We will infer the abundances of a large number of elements, sampling various nucleosynthetic pathways. The includes Fe-peak elements (Fe, Ni, Cr, Mn), α elements (O, Mg, Si, Ca, Ti), light elements (C, N), and odd-Z elements (Al, Na). The distribution of M33 stars on the various chemical planes will constrain the early history of star formation of M33, in a similar way to studies of MW satellites on the basis of APOGEE data (e.g., Hayes et al., 2020; Hasselquist et al., 2021; Fernandes et al., 2023). Finally, radial velocity precision (see below) will be good enough to afford a distinction between halo and disk populations in M33, shedding a first glimmer of light on the earliest episodes of mass assembly of the M33 galaxy.

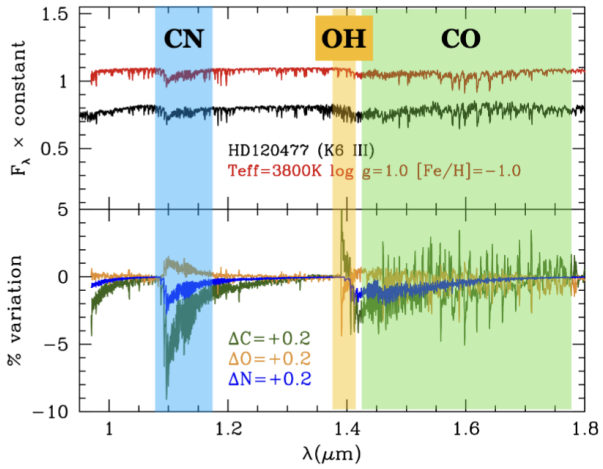

Figure 5: *Top*: Spectrum synthesis based on the MARCS model atmospheres (Gustafsson et al., 2008) and `Synspec` (Hubeny & Lanz, 2017) is a very good match to the IRTF spectrum (Rayner et al., 2009) of a nearby K giant. Although no attempt was made to match the observed spectrum, the comparison illustrates the quality of our spectral analysis package. *Bottom*: Spectral variation as a function of elemental abundances. In both panels shades indicate the positions of main molecular bands. Band strength and sensitivity indicate that C, N, and O abundances can be derived with the required precision on the basis of the estimated S/N. In addition, multiple atomic lines will be easily resolved at the expected metallicity.

Field and target selection: We select targets from the PHATTER survey (Dalcanton et al., 2012). For this pilot study, we target stars located within four mosaics (namely, NN, NW, SS, SW) in Brick B01, located in the north-west quadrant of M33's projected disk. This field has no substantial contamination by spiral arms, low levels of extinction, and is dominated by stars older than ∼1 Gyr. Its location roughly 1.4 scale lengths from the centre of M33 (Regan & Vogel, 1994) means that its stellar populations may contain a non-negligible contribution from the halo of M33 (Gilbert et al., 2022). The WFPC-3 NIR CMD of Brick 01 is shown in Fig. 4. A well defined giant branch above the red clump (F160W≈22) is clearly visible. In order to control for the impact of extra mixing of the C and N abundances along the upper giant branch, as well as other $T_{\rm eff}/\log g$-related systematics, we select targets within a narrow magnitude range (18.7 < F160W < 19.3). According to the PARSEC theoretical isochrones (Marigo et al., 2017), assuming a distance modulus of 24.57, and $A_{\rm F160W}$ ∼0.02 (Conn et al., 2012), stars in this position of the CMD have typically $T_{\rm eff}$∼ 3900 K and log$g$∼ 0.5 for [Fe/H] = –1 and [α/Fe] = 0 (the numbers are fairly insensitive to the assumption on extinction and [α/Fe]). A small amount of AGB contamination in our sample is expected, which will be filtered out on the basis of ^{12}C/^{13}C ratios. In addition to the M33 field, we will obtain spectra for a comparable sample of stars from a well studied cluster, ω Centaurus. Abundance data for ∼ 2,000 stars from ω Cen are publically available from the APOGEE survey (Mészáros et al., 2021) and optical studies (Johnson & Pilachowski, 2010), so that we will have reliable calibrators of our abundance system for the relevant range of metallicities and chemical compositions.

Instrumental setup: Our elemental abundance analysis requires measurement of the strengths of a large number of atomic lines and molecular bands in absorption. Medium resolution spectroscopy, despite not fully resolving absorption lines, has been shown to yield good quality elemental abundances when subject to modern automatic abundance methods (e.g., Allende Prieto, 2004). To achieve our goals we plan to adopt the G140H/F100LP grating/filter combination to cover the $\lambda\lambda$0.9-1.8μm spectral range. Synthetic and observed spectra in that range are displayed in Fig. 5, where the sensitivity of the entire spectral region to the abundances of CNO based molecules is displayed. In addition, tens of measureable atomic lines due to the atomic species of interest are included in this spectral region. Because the PSF of JWST has proved to be better than initially expected, NIRSpec is delivering better spectral resolution (R∼4000-5000) for point sources than the nominal R=2700. Therefore, our abundance analysis approach will consist of the combination of automatic

minimization against a huge synthetic spectral library (already calculated) based on state of the art model atmospheres and line lists, and a classical abundance analysis to ascertain the fidelity of the automatic approach. Preliminary results on the analysis of NIRSPec spectra, obtained using the same setup as adopted in this proposal, for a calibration cluster star show excellent results (Fig. **??**).

Because of the sharp PSF delivered by the JWST optical system, the projected line spread function of the NIRSpec spectra is severely undersamples (FWHM$\sim$1pixel). To mitigate this problem our observational design includes subpixel dithers in the dispersion direction. To keep every star within the slitlet for every exposure we adopt a "Constrained" source centering constraint. We expect our data not to be background dominated, so we adopt 1 Shutter Slitlet design. In addition addition to cross dispersion dithers aimed at minimizing the impact of detector response features.

S/N and Exposure time requirements The strength of the spectral features we need to measure, as well as their dependence on various elemental abundance variations (Fig. 5) mandate a high S/N/pixel. A detailed mapping of the distribution of M33's stellar populations in the α-Fe plane requires abundance precisions of the order of $\sim$0.1 dex. The ETC (Workbook ID 142613) tells us that, for a star with F160W=19 we obtain S/N/pixel=100 at 1.15μm, adopting 20 groups/integration, 4 integrations/exposure, and a total of 4 exposures, with a NRSIRS2 readout pattern. Exposure patterns were adjusted to obtain similar S/N for ω Cen stars. Preimaging is requested for both sets of observations (M33 and calibration cluster).

Special Requirements (if any)

Justify Coordinated Parallel Observations (if any)

Justify Duplications (if any)

Analysis Plan (AR only)

References

Allende Prieto C., 2004, Astronomische Nachrichten, 325, 604

Andrews B. H., Weinberg D. H., Schönrich R., Johnson J. A., 2017, ApJ, 835, 224

Beasley M. A., San Roman I., Gallart C., Sarajedini A., Aparicio A., 2015, MNRAS, 451, 3400

Blanton M. R., 2006, ApJ, 648, 268

Block D. L., Freeman K. C., Jarrett T. H., Puerari I., Worthey G., Combes F., Groess R., 2004, A&A, 425, L37

Brinchmann J., Charlot S., White S. D. M., Tremonti C., Kauffmann G., Heckman T., Brinkmann J., 2004, MNRAS, 351, 1151

Bundy K., et al., 2006, ApJ, 651, 120

Carrera R., Gallart C., Hardy E., Aparicio A., Zinn R., 2008, AJ, 135, 836

Cioni M. R. L., 2009, A&A, 506, 1137

Conn A. R., et al., 2012, ApJ, 758, 11

Corbelli E., Walterbos R. A. M., 2007, ApJ, 669, 315

Cowie L. L., Songaila A., Hu E. M., Cohen J. G., 1996, AJ, 112, 839

Crockett N. R., Garnett D. R., Massey P., Jacoby G., 2006, ApJ, 637, 741

Dalcanton J. J., et al., 2012, ApJS, 200, 18

Elmegreen B. G., Elmegreen D. M., Montenegro L., 1992, ApJS, 79, 37

Faber S. M., et al., 2007, ApJ, 665, 265

Fernandes L., et al., 2023, MNRAS, 519, 3611

Garnett D. R., Odewahn S. C., Skillman E. D., 1992, AJ, 104, 1714

Gebek A., Matthee J., 2022, ApJ, 924, 73

Gilbert K. M., et al., 2022, ApJ, 924, 116

Goddard D., et al., 2017, MNRAS, 466, 4731

Governato F., et al., 2015, MNRAS, 448, 792

Gustafsson B., Edvardsson B., Eriksson K., Jørgensen U. G., Nordlund Å., Plez B., 2008, A&A, 486, 951

Hasselquist S., et al., 2021, ApJ, 923, 172

Hayden M. R., et al., 2015, ApJ, 808, 132

Hayes C. R., et al., 2020, ApJ, 889, 63

Hendricks B., Koch A., Lanfranchi G. A., Boeche C., Walker M., Johnson C. I., Peñarrubia J., Gilmore G., 2014, ApJ, 785, 102

Horta D., et al., 2021, MNRAS, 500, 5462

Horta D., et al., 2022, MNRAS,

Hubeny I., Lanz T., 2017, arXiv e-prints, p. arXiv:1706.01859

Johnson C. I., Pilachowski C. A., 2010, ApJ, 722, 1373

Johnson J. W., et al., 2021, MNRAS, 508, 4484

Kauffmann G., et al., 2003, MNRAS, 341, 33

Koch A., Grebel E. K., Martell S. L., 2019, A&A, 625, A75

Kormendy J., McClure R. D., 1993, AJ, 105, 1793

Kwitter K. B., Aller L. H., 1981, MNRAS, 195, 939

Mackereth J. T., et al., 2017, MNRAS, 471, 3057

Maoz D., Graur O., 2017, ApJ, 848, 25

Marigo P., et al., 2017, ApJ, 835, 77

Martig M., Minchev I., Ness M., Fouesneau M., Rix H.-W., 2016, ApJ, 831, 139

Martín-Navarro I., 2016, MNRAS, 456, L104

Martin D. C., et al., 2007, ApJS, 173, 342

Matteucci F., Greggio L., 1986, A&A, 154, 279

McCarthy J. K., Lennon D. J., Venn K. A., Kudritzki R.-P., Puls J., Najarro F., 1995, ApJ, 455, L135

McLean I. S., Liu T., 1996, ApJ, 456, 499

McWilliam A., 1997, ARA&A, 35, 503

Mészáros S., et al., 2021, MNRAS, 505, 1645

Monteverde M. I., Herrero A., Lennon D. J., Kudritzki R. P., 1997, ApJ, 474, L107

Monteverde M. I., Herrero A., Lennon D. J., 2000, ApJ, 545, 813

Muñoz-Mateos J. C., Gil de Paz A., Boissier S., Zamorano J., Jarrett T., Gallego J., Madore B. F., 2007, ApJ, 658, 1006

Ness M., Hogg D. W., Rix H. W., Martig M., Pinsonneault M. H., Ho A. Y. Q., 2016, ApJ, 823, 114

Nidever D. L., et al., 2020, ApJ, 895, 88

Noeske K. G., et al., 2007, ApJ, 660, L43

Peña M., Flores-Durán S. N., 2019, Rev. Mexicana Astron. Astrofis., 55, 255

Rayner J. T., Cushing M. C., Vacca W. D., 2009, ApJS, 185, 289

Regan M. W., Vogel S. N., 1994, ApJ, 434, 536

Rosolowsky E., Simon J. D., 2008, ApJ, 675, 1213

Rybizki J., Just A., Rix H.-W., 2017, A&A, 605, A59

Salaris M., Pietrinferni A., Piersimoni A. M., Cassisi S., 2015, A&A, 583, A87

Salim S., et al., 2007, ApJS, 173, 267

Searle L., 1971, ApJ, 168, 327

Tinsley B. M., 1979, ApJ, 229, 1046

Tollerud E. J., Boylan-Kolchin M., Barton E. J., Bullock J. S., Trinh C. Q., 2011, ApJ, 738, 102

Tolstoy E., Hill V., Tosi M., 2009, ARA&A, 47, 371

Urbaneja M. A., Herrero A., Kudritzki R. P., Najarro F., Smartt S. J., Puls J., Lennon D. J., Corral L. J., 2005, ApJ, 635, 311

Vilchez J. M., Pagel B. E. J., Diaz A. I., Terlevich E., Edmunds M. G., 1988, MNRAS, 235, 633

Walcher C. J., Coelho P. R. T., Gallazzi A., Bruzual G., Charlot S., Chiappini C., 2015, A&A, 582, A46

Williams B. F., Dalcanton J. J., Dolphin A. E., Holtzman J., Sarajedini A., 2009, ApJ, 695, L15

Williams B. F., et al., 2021, ApJS, 253, 53

Worthey G., Faber S. M., Gonzalez J. J., 1992, ApJ, 398, 69

Zahid H. J., Dima G. I., Kewley L. J., Erb D. K., Davé R., 2012, ApJ, 757, 54

Zheng Z., et al., 2019, ApJ, 873, 63

van der Marel R. P., Alves D. R., Hardy E., Suntzeff N. B., 2002, AJ, 124, 2639

van der Marel R. P., Besla G., Cox T. J., Sohn S. T., Anderson J., 2012, ApJ, 753, 9